

Spin accumulation from nonequilibrium first principles methodsAlexander Fabian,^{*} Michael Czerner, and Christian Heiliger*Institute for Theoretical Physics, Justus Liebig University Giessen, Heinrich-Buff-Ring 16, 35392 Giessen, Germany
and Center for Materials Research (LaMa), Justus Liebig University Giessen, Heinrich-Buff-Ring 16, 35392 Giessen, Germany*Hugo Rossignol[✉] and Ming-Hung Wu*HH Wills Physics Laboratory, University of Bristol, Tyndall Avenue, Bristol BS8 1TL, United Kingdom*

Martin Gradhand

*HH Wills Physics Laboratory, University of Bristol, Tyndall Avenue, Bristol BS8 1TL, United Kingdom
and Institute of Physics, Johannes Gutenberg University Mainz, 55099 Mainz, Germany*

(Received 11 March 2021; accepted 19 July 2021; published 2 August 2021)

For the technologically relevant spin Hall effect, most theoretical approaches rely on the evaluation of the spin-conductivity tensor. In contrast, for most experimental configurations the generation of spin accumulation at interfaces and surfaces is the relevant quantity. Here, we directly calculate the accumulation of spins due to the spin Hall effect at the surface of a thin metallic layer, making quantitative predictions for different materials. Two distinct limits are considered, both relying on a fully relativistic Korringa-Kohn-Rostoker density functional theory method. In the semiclassical approach, we use the Boltzmann transport formalism and compare it directly with a fully quantum mechanical nonequilibrium Keldysh formalism. Restricting the calculations to the spin-Hall-induced, odd-in-spatial-inversion, contribution in the limit of the relaxation time approximation, we find good agreement between the two methods, where deviations can be attributed to the complexity of Fermi surfaces. Finally, we compare our results with experimental values of the spin accumulation at surfaces as well as the Hall angle and find good agreement for the trend across the considered elements.

DOI: [10.1103/PhysRevB.104.054402](https://doi.org/10.1103/PhysRevB.104.054402)**I. INTRODUCTION**

The spin Hall effect was first proposed in 1971 by Dyakonov and Perel [1]. Only after Hirsch [2] re-established the concept in 1999 was it experimentally observed directly in semiconductors by Kato *et al.* [3] and Wunderlich *et al.* [4]. The spin Hall effect enables the generation of spin current in nonmagnetic materials by passing an electric current through a system opening the route to various applications in spintronics [5–12]. Importantly, the inverse effect, generating a charge current from a spin current, or in fact a spin accumulation, gives a tool to detect spin currents electronically [13–15].

The origin of the effect is commonly divided into two contributions, the intrinsic [16–19] and the extrinsic mechanism. While the first derives from the intrinsic spin-orbit coupling of the pure material, the latter is mediated via spin-orbit coupling at an impurity site. For the extrinsic process, the skew or Mott scattering dominates in the dilute limit [20,21], and the side jump [22] scales similarly to the intrinsic mechanism with the sample resistivity.

One can approach the spin Hall effect theoretically typically via semiclassical or fully quantum mechanical approaches. In the case of the semiclassical theory, the intrinsic mechanism is recast in terms of the Berry cur-

vature [18,23,24], and the extrinsic, almost exclusively the skew scattering mechanism, is considered via a Boltzmann equation incorporating the vertex corrections (scattering-in term) [25–27]. On the other hand, the Kubo or Kubo-Streda (Kubo-Bastin) formalism has been used to consider the intrinsic mechanism [28,29], or in combination with the coherent potential approximation the extrinsic mechanisms were included on an equal footing [30]. However, all approaches have in common that they almost exclusively calculate the spin Hall conductivity in a periodic crystal [31–33], giving no direct access to the spin accumulation at surfaces or interfaces. In contrast, most experimental configurations will rely on the accumulation at interfaces and surfaces exploiting spin diffusion equations in order to extract the spin Hall conductivity [3,34,35]. However, the induced spin accumulation has attracted renewed interest as the technologically relevant spin-orbit torque often relies on spin accumulation at, as well as spin currents through, normal metal ferromagnet interfaces [36–40]. Experimentally, it is incredibly difficult to distinguish the various contributions, rendering it a challenge to optimize spin-orbit materials and the corresponding bilayer systems [41,42].

In this paper, we directly calculate the spin accumulation induced at the surfaces of metallic thin films when a charge current is passed through the sample. We focus on the contributions with the same symmetry as the spin Hall effect, namely, the spin accumulation which is odd under spatial

^{*}Alexander.Fabian@physik.uni-giessen.de

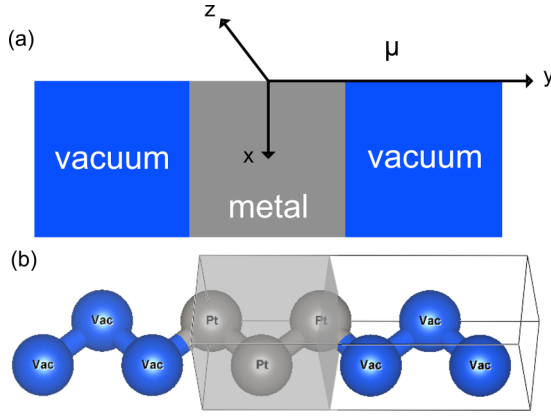


FIG. 1. (a) Schematic drawing of the slab systems for the Keldysh formalism. The atomic index counts the atoms along the y direction. (b) Actual unit cell for fcc Pt. For the Keldysh formalism the box indicates the supercell. For the Boltzmann formalism the vacuum is extended into the semi-infinite half-spaces on both sides of the slab (not shown).

inversion [36–38], showing equal and opposite spin accumulations at the two surfaces of the thin metallic film. For that reason, we deliberately omit the even-under-spatial-inversion part of the accumulation. This will allow us to make contact with experimental observations and theoretical predictions of the spin Hall effect in more realistic geometries. The system is shown in Fig. 1(a), where a charge current is driven in the z direction, the spin is pointing along x , and the accumulation is calculated in the y direction perpendicular to the plane of the thin film. As the atomic configuration is preserving inversion symmetry and we focus on the contributions from the clean system, it is the Fermi-surface-driven and odd-under-spatial-inversions contribution [36,37], which is linear in the applied longitudinal current, for which we make quantitative predictions in a series of metallic systems. On the one hand, we go beyond the semiclassical approach [38] previously applied to bilayer systems using a fully quantum mechanical Keldysh formalism based on nonequilibrium Green’s functions. On the other hand, we apply this formalism to real materials in a fully *ab initio* density functional theory (DFT) framework going a step further than earlier works on the spin accumulation in nonequilibrium description which were restricted to a model Hamiltonian [43,44]. To validate our method, we compare it with a semiclassical approach relying on the Boltzmann formalism.

After a brief introduction of both methods we will present exemplary results and compare the induced spin accumulation with experimental findings. Furthermore, we will analyze the common trends across the elements with respect to the charge-to-spin-current conversion efficiency.

II. THEORY

The electronic structure is calculated via a fully relativistic Korringa-Kohn-Rostoker (KKR) density functional theory method [45]. Both band structure methods, for the semiclassical approach [46,47] and the Keldysh formalism [48–50], have been introduced earlier. Here, we only highlight the

adjustments and relevant expressions used to express the steady-state magnetization density.

A. Keldysh formalism

For the Keldysh formalism the system is divided into three parts, the left (L), center (C), and right (R) regions. The left and right parts work as semi-infinite leads in equilibrium with the same Fermi levels E_F . Their influence on the center region is accounted for by the corresponding self-energies $\Sigma_{L/R}$. When applying a bias voltage, the levels of the chemical potential change to $\eta_{>/<} = E_F \pm \frac{e\Delta\varphi}{2}$ accordingly. In the range of $[\eta_{<}, \eta_{>}]$ the fully relativistic electron density and magnetization density are calculated as [45]

$$\rho(\vec{r}) = \frac{1}{2\pi} \int_{\eta_{<}}^{\eta_{>}} \langle \vec{r} | \text{Tr}[G(E)\Gamma(E)G^\dagger(E)] | \vec{r} \rangle dE, \quad (1)$$

$$m^{(i)}(\vec{r}) = \frac{\mu_B}{2\pi} \int_{\eta_{<}}^{\eta_{>}} \langle \vec{r} | \text{Tr}[\beta \zeta_i G(E)\Gamma(E)G^\dagger(E)] | \vec{r} \rangle dE, \quad (2)$$

respectively. Here, $G(E)$ is the Green’s function of the center area, and $\Gamma = i[\Sigma(E) - \Sigma^\dagger(E)]$ is the broadening function, where $\Sigma(E) = \Sigma_L(E) + \Sigma_R(E)$,

$$\beta = \begin{pmatrix} I_2 & 0 \\ 0 & -I_2 \end{pmatrix}, \quad \zeta_i = \begin{pmatrix} \sigma_i & 0 \\ 0 & \sigma_i \end{pmatrix},$$

I_2 is the 2×2 unity matrix, and σ_i are the Pauli spin matrices with $i \in \{x, y, z\}$. In the so-called one-shot calculations, only the magnetization at the Fermi level is considered for vanishing bias voltage, which is

$$m_i(\vec{r}) = \frac{\mu_B}{2\pi} \text{Tr}[\beta \zeta_i G(E_F)\Gamma(E_F)G^\dagger(E_F)]e\Delta\varphi.$$

Finally, the magnetic moment due to spin accumulation $a_x(\mu)$ is evaluated by integrating $m_x(\vec{r})$ over the volume V_μ of the atomic sphere at atomic index μ :

$$a_x(\mu) = \int_{V_\mu} m_x(\vec{r}) dV. \quad (3)$$

The current density is calculated via the Landauer-Büttiker formula in the case of a vanishing bias voltage [51]

$$j_z = \frac{e^2}{A\hbar} T(E_F)\Delta\varphi \quad (4)$$

assuming that the transmission $T(E) = \text{Tr}[\Gamma_L G \Gamma_R G^\dagger]$ is nearly constant in the range of $\Delta E = e\Delta\varphi$. Here, A is the area of the supercell in the x and y directions.

B. Boltzmann formalism

Within the Boltzmann formalism the spin accumulation is expressed as a Fermi surface integral [38]. For two-dimensional (2D) systems the spin accumulation is expressed as [52]

$$\vec{a} = \chi_\mu \cdot \vec{E} = -\frac{e\mu_B}{\hbar} \frac{V}{d(2\pi)^2} \int_{E_F} \frac{dl}{|v_{\vec{k}}|} (\vec{s}_{\vec{k}}(\mu) \circ \tau_{\vec{k}} v_{\vec{k}}) \cdot \vec{E}, \quad (5)$$

where V is the volume of the cell, d is the thickness of the film, $v_{\vec{k}}$ is the group velocity at \vec{k} , $\vec{s}_{\vec{k}}$ is the expectation value of the spin operator, and \vec{E} is the applied electric field.

Because of degenerate states, the spin operator exhibits off-diagonal elements. A gauge transformation is applied, such that these off-diagonal elements vanish. The current density is given by

$$\vec{j} = \underline{\sigma} \cdot \vec{E} = -\frac{e^2}{\hbar} \frac{1}{d(2\pi)^2} \int_{E_F} \frac{dl}{|\vec{v}_{\vec{k}}|} (\vec{v}_{\vec{k}} \circ \tau_{\vec{k}} \vec{v}_{\vec{k}}) \cdot \vec{E}. \quad (6)$$

Importantly, both scale linearly with the relaxation time. In the chosen geometry, $\vec{j} = j\vec{e}_z$ and $\vec{E} = E_z\vec{e}_z$, and by using the relaxation time approximation $\tau_{\vec{k}} = \tau$, the relevant expressions can be simplified as

$$a_x(\mu) = \chi_{xz} E_z = \frac{e}{\hbar} \frac{\mu_B V \tau E_z}{d(2\pi)^2} \int_{E_F} \frac{dl}{|\vec{v}_{\vec{k}}|} s_{x,\vec{k}}(\mu) v_{z,\vec{k}} \quad (7)$$

and

$$j_z = \frac{e^2}{\hbar} \frac{\tau E_z}{d(2\pi)^2} \int_{E_F} \frac{v_{z,\vec{k}} v_{z,\vec{k}}}{|\vec{v}_{\vec{k}}|} dl = \frac{e^2}{\hbar} \frac{\tau E_z}{d(2\pi)^2} \langle v_z^2 \rangle. \quad (8)$$

This maneuver will allow us to remove the direct dependence of the spin accumulation on the relaxation time τE_z , replacing it with the current density

$$\frac{a_x(\mu)}{\mu_B} = \frac{j_z}{e} \frac{V}{\langle v_z^2 \rangle} \int_{E_F} \frac{dl}{|\vec{v}_{\vec{k}}|} s_{x,\vec{k}}(\mu) v_{z,\vec{k}}. \quad (9)$$

Thus the spin accumulation will scale linearly with the current density, which, in turn, can be calculated within the Keldysh formalism. This will allow for direct mapping between the two methods.

C. Computational details

For the Keldysh formalism the starting point consists of self-consistently calculated equilibrium potentials, which are obtained in a supercell approach including atomic spheres and vacuum spheres to form the thin film geometry. For the transport calculations, the supercell is connected to semi-infinite leads from the left and right sides along the transport direction (z direction). The corresponding cells are schematically shown in Fig. 1. In the following, a one-step nonequilibrium Keldysh formalism at the Fermi energy is used to find the steady-state densities from these potentials. The applied

voltage is chosen to be reasonably small at $\Delta\varphi = 10^{-4}$ Ry/ e , in order to agree with the approximation of vanishing applied electric field in the linear response regime as assumed in the Boltzmann approach.

For the Boltzmann formalism the construction is based on a slab calculation with semi-infinite vacuum attached perpendicular to the film. After obtaining the self-consistent potentials, the Fermi surface parameters such as the \vec{k} -resolved band velocities and spin expectation values are calculated to find the spin accumulation according to Eq. (9). Given the linear scaling of the spin accumulation with the current density in the Boltzmann formalism, we insert the current density found within the Keldysh approach to facilitate direct comparison.

Within the Landauer-Büttiker approach the finite conductance stems from a contact resistance at the interfaces of the leads. This contact resistance is also often referred to as Sharvin resistance [53]. Naturally, it does not depend on the length of the transport system; rather, it depends only on the number of available transport channels. In contrast, for the Boltzmann approach the contact resistance is ignored, and the whole resistance originates from scattering in the volume. In our comparison we adjust j such that it fits the Sharvin resistance of the Landauer-Büttiker approach. As such, the mechanism for the finite currents is different in both approaches; however, the resulting current density itself is the same, driving the spin accumulation at the surfaces. We do not account for any extrinsic mechanisms; rather, we only account for contributions to accumulation arising from the electronic structure of the clean crystal.

As we apply a bias in the z direction, the only relevant element of the spin accumulation in the considered cubic systems is $a_x(\mu)$, and for convenience we are going to omit the index x in the following. The axes of the coordinate systems are aligned parallel to the $\langle 100 \rangle$ axes of the crystals.

III. RESULTS AND DISCUSSION

The resulting spin accumulation $a(\mu)$ as a function of the atomic position index μ is shown in Fig. 2 for the fcc (Cu, Pt) [Fig. 2(a)] and bcc (Ta, U) [Fig. 2(b)] systems comparing

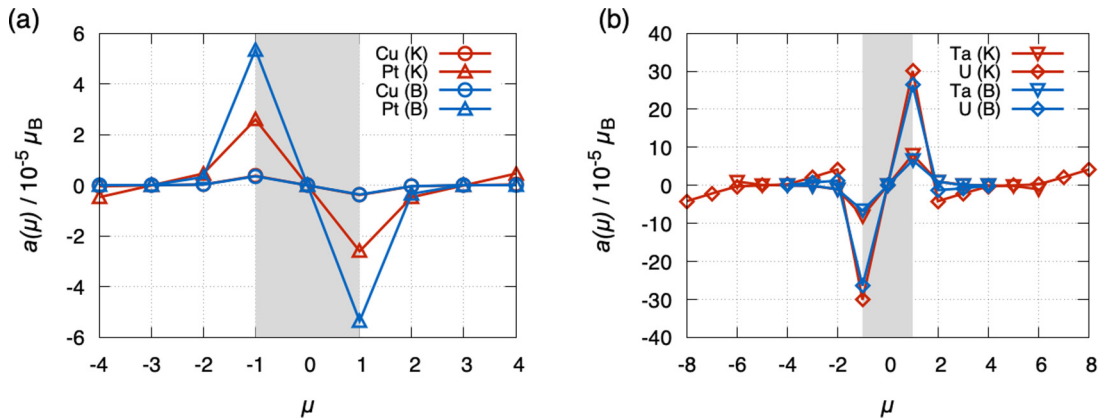


FIG. 2. Magnetic moment per atom for representative (a) fcc systems and (b) bcc systems. Blue refers to Keldysh (K) calculated values, and red refers to Boltzmann (B) calculated values. The thin film is highlighted in gray. Each line shows the same antisymmetric behavior. Note that in (a) the Keldysh and Boltzmann values for Cu overlap.

TABLE I. First extrema of the spin accumulation calculated by Boltzmann and Keldysh formalisms as well as the Keldysh current density for the small systems. Comparison between a/j and spin Hall angle $\theta_{\text{SH}}^{\text{exp}}$ [54]. Intrinsic spin Hall conductivities from calculations are shown for reference.

Element	$a(\mu = -1)$ ($10^{-6} \mu_{\text{B}}$)		j (10^{12} A/m^2)	a/j ($10^{-17} \mu_{\text{B}} \text{ A}^{-1} \text{ m}^2$)		$\theta_{\text{SH}}^{\text{exp}}$ [54] (%)	$\sigma_{\text{SH}}^{\text{theo}}$ ($(\hbar/e) \Omega^{-1} \text{ cm}^{-1}$)
	Boltzmann	Keldysh		Boltzmann	Keldysh		
Cu (fcc)	3.60	3.77	1.50	0.24	0.25	0.32	
Ag (fcc)	2.65	2.41	1.16	0.23	0.21	0.68	
Au (fcc)	17.62	16.33	1.33	1.32	1.23	8.4	400 [31]
Ta (bcc)	-66.19	-80.99	1.17	-5.66	-6.92	-7.1	-142 [55]
Pd (fcc)	31.33	10.10	1.12	2.80	0.90		1400 [31]
Pt (fcc)	53.53	25.99	1.79	2.99	1.45	10.00	2000 [17]
U (bcc)	-263.9	-300.9	1.93	-13.7	-15.6		-402 [56]

the Keldysh (K) and Boltzmann (B) formalisms, respectively. The position index is chosen such that the central atom of the film is labeled as 0. The general behavior is the same for all considered elements as well as between the two methods. This is largely enforced by symmetry since atoms $\mu = \pm 1$ have equal and opposite spin accumulation. For easier comparison we summarize the maximum spin accumulation $a(\mu = -1)$ for the various systems as well as the two methods in Table I. As expected, the spin accumulation increases with increasing atomic weight corresponding to enhanced spin-orbit coupling. While this is true in general, it is not correct in the details. The spin accumulation for Ag is smaller than that for Cu, and for Ta we find a surprisingly large spin accumulation. Such details would be difficult to predict from simplified models. Comparing the Boltzmann formalism with the Keldysh formalism, the agreement is perfect for the noble metals, with their simple Fermi surfaces, but starts to deviate for the more complex systems of Ta, Pd, Pt, and U. Nevertheless, the sign as well as the overall magnitude is still in remarkable agreement.

We believe this correlation between Fermi surface complexity (see Fig. S5 in the Supplemental Material [57]) and the agreement between the two methods not to be a numerical artifact. In the Keldysh formalism we only consider the ballistic transport, where each band contributes equally to the electronic transport. In contrast, the Boltzmann formalism relies on electron scattering, and the weighting in any Fermi surface integral will depend on the \vec{k} -dependent band velocity in the transport direction. For more complex structures the variations in the absolute value of the band velocity on the Fermi surface are much more pronounced (Ta, U, Pd, Pt) than for the simple metals Au, Ag, and Cu (see Fig. S5 in the Supplemental Material [57]). For elements with simple Fermi surfaces and subsequently the least-changing Fermi velocity, the results obtained within the Boltzmann formalism nevertheless match well.

So far we have considered rather thin layers with limited access to the decay length of the spin accumulation within the thin film. To investigate this point further, we consider three larger systems, Cu, Pt, and U, with nine layers of atoms (cf. Fig. 3 and also the Supplemental Material [57]). For Cu the decay of the spin accumulation is remarkably strong, happening within three layers, and is in excellent agreement between the two methods. In contrast, the decay appears to be much slower for Pt and even more so for U {see Fig. S3(c)

in the Supplemental Material [57]}, again consistent between the two methods.

In order to validate our results, we compare them with recent experiments where the spin accumulation of Pt thin films was directly measured by the magneto-optic Kerr effect (MOKE) [34]. In that experiment a strong thickness dependence was established with a value of $a/j = 5 \times 10^{-16} \mu_{\text{B}} \text{ A}^{-1} \text{ m}^2$ for samples with a thickness $t > 40 \text{ nm}$. Extrapolating the experimental data Eq. (1) in Ref. [34] to the film thickness of $t = 0.39 \text{ nm}$ considered here yields a result of $a/j = 1.05 \times 10^{-17} \mu_{\text{B}} \text{ A}^{-1} \text{ m}^2$ in rather good agreement with our result of $a/j = 1.45 \times 10^{-17} \mu_{\text{B}} \text{ A}^{-1} \text{ m}^2$. While measurements of spin Hall angles and spin Hall conductivities are widely available, to our knowledge, such direct numerical measurements of the spin accumulation for other systems are very sparse. It is therefore difficult to compare the results from our methods directly with literature values. It appears natural to compare them with spin Hall conductivities or spin Hall angles predicted theoretically or measured experimentally. However, this holds multiple caveats. For example, theoretically predicted intrinsic conductivities are bulk calculations ignoring the fact that any spin accumulation will depend on the actual surface geometry and film thickness. While sign changes and overall magnitudes ought to be in agreement, significant variations are possible in the details. As summarized in Table I the signs are in agreement between

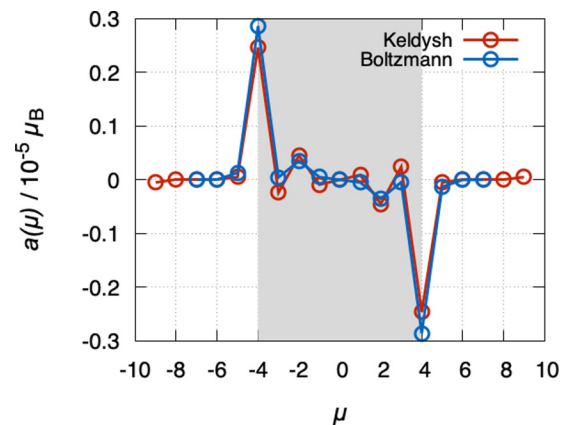


FIG. 3. Magnetization for a thin film of nine Cu atoms (highlighted in gray).

the spin accumulations and the intrinsic spin Hall conductivities, but the high spin accumulation for Ta and U cannot trivially be predicted from the conductivities. On the other hand, experimental results for the spin Hall angles tend to vary significantly over the various experimental techniques and sample preparations, which will often involve different nonmagnetic-ferromagnetic (NM-FM) interfaces [58] and varying degrees of extrinsic mechanisms contributing to the overall effect [59]. Consequently, any comparison should focus on one technique with similar sample preparation only. Choosing a spin pumping experiment in which most of the considered metals were investigated under similar conditions [54], the trend for a/j and $\theta_{\text{SH}}^{\text{exp}}$ in Table I is quite consistent for systems with simpler Fermi surfaces (Cu, Ag, Au). Similarly, Ta, Au, and Pt show increasing spin Hall angles in the same order of magnitude, with a sign change occurring for Ta. This sign change cannot be trivially predicted for multibanded systems, since the spin-orbit coupling depends on the orbital and on the Fermi level [55].

IV. CONCLUSION

We extended existing theoretical frameworks to capture the spin-Hall-effect-induced spin accumulation in various metallic thin films via a fully nonequilibrium Keldysh formalism. We tested this new approach against a linearized Boltzmann approach as well as experimental findings and found remarkable agreement in all cases, reproducing all sign changes and predicting the same trends. Where the two theoretical approaches differ most is the atom-resolved spin accumulation in thicker films especially for systems with complex Fermi surfaces, whereas for Cu we find an excellent agreement. This methodology will enable us to make more direct con-

tact with experiments, where instead of the conductivities derived from periodic crystals it is the spin accumulation at interfaces and surfaces as well as the spin current through interfaces which are the relevant driving mechanisms of, for example, magnetization reversal in ferromagnets. In this first and most important step we have established that the developed methodology reproduces the spin-Hall-induced spin accumulation in the thin metallic films well across different frameworks and in comparison to experiment. This will open up broad opportunities to explore the effect in more complex interfaces as well as under the influence of impurities, making even more direct contact with experimental realities. Incorporating inversion asymmetry and contributions even under spatial inversion symmetry [36,37] will give access to spin galvanic effects [60] while investigating the additional influence of impurities and the additional Mott scattering [39]. In all these cases, the full nonequilibrium description adds additional complexity with the possibility of finite bias across the sample geometry.

ACKNOWLEDGMENTS

A.F., M.C., and C.H. acknowledge computational resources provided by the HPC Core Facility and the HRZ of the Justus Liebig University Giessen. Furthermore, they would like to thank Marcel Giar and Philipp Risius of HPC-Hessen, funded by the State Ministry of Higher Education, Research and the Arts, for technical support. M.-H.W., H.R., and M.G. carried out their computational work using the computational facilities of the Advanced Computing Research Centre, University of Bristol. M.G. thanks the visiting professorship program of the Centre for Dynamics and Topology at Johannes Gutenberg University Mainz.

-
- [1] M. I. Dyakonov and V. I. Perel, *Phys. Lett. A* **35**, 459 (1971).
 - [2] J. E. Hirsch, *Phys. Rev. Lett.* **83**, 1834 (1999).
 - [3] Y. K. Kato, R. C. Myers, A. C. Gossard, and D. D. Awschalom, *Science* **306**, 1910 (2004).
 - [4] J. Wunderlich, B. Kaestner, J. Sinova, and T. Jungwirth, *Phys. Rev. Lett.* **94**, 047204 (2005).
 - [5] S. Fukami, T. Anekawa, C. Zhang, and H. Ohno, *Nat. Nanotechnol.* **11**, 621 (2016).
 - [6] Y. V. Pershin, N. A. Sinitsyn, A. Kogan, A. Saxena, and D. L. Smith, *Appl. Phys. Lett.* **95**, 022114 (2009).
 - [7] A. Hoffmann, *IEEE Trans. Magn.* **49**, 5172 (2013).
 - [8] L. Liu, C.-F. Pai, Y. Li, H. W. Tseng, D. C. Ralph, and R. A. Buhrman, *Science* **336**, 555 (2012).
 - [9] Y. Kajiwara, K. Harii, S. Takahashi, J. Ohe, K. Uchida, M. Mizuguchi, H. Umezawa, H. Kawai, K. Ando, K. Takanashi, S. Maekawa, and E. Saitoh, *Nature (London)* **464**, 262 (2010).
 - [10] H. Nakayama, M. Althammer, Y.-T. Chen, K. Uchida, Y. Kajiwara, D. Kikuchi, T. Ohtani, S. Geprägs, M. Opel, S. Takahashi, R. Gross, G. E. W. Bauer, S. T. B. Goennenwein, and E. Saitoh, *Phys. Rev. Lett.* **110**, 206601 (2013).
 - [11] H. Wu, X. Zhang, C. H. Wan, B. S. Tao, L. Huang, W. J. Kong, and X. F. Han, *Phys. Rev. B* **94**, 174407 (2016).
 - [12] K. Ando, S. Takahashi, K. Harii, K. Sasage, J. Ieda, S. Maekawa, and E. Saitoh, *Phys. Rev. Lett.* **101**, 036601 (2008).
 - [13] S. O. Valenzuela and M. Tinkham, *Nature (London)* **442**, 176 (2006).
 - [14] H. Zhao, E. J. Loren, H. M. van Driel, and A. L. Smirl, *Phys. Rev. Lett.* **96**, 246601 (2006).
 - [15] E. Saitoh, M. Ueda, H. Miyajima, and G. Tatara, *Appl. Phys. Lett.* **88**, 182509 (2006).
 - [16] J. Sinova, D. Culcer, Q. Niu, N. A. Sinitsyn, T. Jungwirth, and A. H. MacDonald, *Phys. Rev. Lett.* **92**, 126603 (2004).
 - [17] G. Y. Guo, S. Murakami, T.-W. Chen, and N. Nagaosa, *Phys. Rev. Lett.* **100**, 096401 (2008).
 - [18] S. Murakami, *Science* **301**, 1348 (2003).
 - [19] J. Sinova, S. O. Valenzuela, J. Wunderlich, C. H. Back, and T. Jungwirth, *Rev. Mod. Phys.* **87**, 1213 (2015).
 - [20] J. Smit, *Physica* **21**, 877 (1955).
 - [21] J. Smit, *Physica* **24**, 39 (1958).
 - [22] L. Berger, *Phys. Rev. B* **2**, 4559 (1970).
 - [23] R. Karplus and J. M. Luttinger, *Phys. Rev.* **95**, 1154 (1954).
 - [24] T. Jungwirth, Q. Niu, and A. H. MacDonald, *Phys. Rev. Lett.* **88**, 207208 (2002).
 - [25] J. C. Swihart, W. H. Butler, G. M. Stocks, D. M. Nicholson, and R. C. Ward, *Phys. Rev. Lett.* **57**, 1181 (1986).

- [26] P. Zahn, J. Binder, and I. Mertig, *Phys. Rev. B* **68**, 100403(R) (2003).
- [27] M. Gradhand, D. V. Fedorov, P. Zahn, and I. Mertig, *Phys. Rev. Lett.* **104**, 186403 (2010).
- [28] G. Y. Guo, Y. Yao, and Q. Niu, *Phys. Rev. Lett.* **94**, 226601 (2005).
- [29] Y. Yao and Z. Fang, *Phys. Rev. Lett.* **95**, 156601 (2005).
- [30] S. Lowitzer, M. Gradhand, D. Ködderitzsch, D. V. Fedorov, I. Mertig, and H. Ebert, *Phys. Rev. Lett.* **106**, 056601 (2011).
- [31] G. Y. Guo, *J. Appl. Phys. (Melville, NY)* **105**, 07C701 (2009).
- [32] X. Wang, J. R. Yates, I. Souza, and D. Vanderbilt, *Phys. Rev. B* **74**, 195118 (2006).
- [33] Y. Yao, L. Kleinman, A. H. MacDonald, J. Sinova, T. Jungwirth, D.-s. Wang, E. Wang, and Q. Niu, *Phys. Rev. Lett.* **92**, 037204 (2004).
- [34] C. Stamm, C. Murer, M. Berritta, J. Feng, M. Gabureac, P. M. Oppeneer, and P. Gambardella, *Phys. Rev. Lett.* **119**, 087203 (2017).
- [35] S. Zhang, *Phys. Rev. Lett.* **85**, 393 (2000).
- [36] F. Freimuth, S. Blügel, and Y. Mokrousov, *Phys. Rev. B* **90**, 174423 (2014).
- [37] S. Wimmer, K. Chadova, M. Seemann, D. Ködderitzsch, and H. Ebert, *Phys. Rev. B* **94**, 054415 (2016).
- [38] G. Géranton, B. Zimmermann, N. H. Long, P. Mavropoulos, S. Blügel, F. Freimuth, and Y. Mokrousov, *Phys. Rev. B* **93**, 224420 (2016).
- [39] D. Ködderitzsch, K. Chadova, and H. Ebert, *Phys. Rev. B* **92**, 184415 (2015).
- [40] A. Kosma, P. Rüßmann, S. Blügel, and P. Mavropoulos, *Phys. Rev. B* **102**, 144424 (2020).
- [41] M. Yang, K. Cai, H. Ju, K. W. Edmonds, G. Yang, S. Liu, B. Li, B. Zhang, Y. Sheng, S. Wang, Y. Ji, and K. Wang, *Sci. Rep.* **6**, 20778 (2016).
- [42] C. O. Avci, K. Garello, C. Nistor, S. Godey, B. Ballesteros, A. Mugarza, A. Barla, M. Valvidares, E. Pellegrin, A. Ghosh, I. M. Miron, O. Boule, S. Auffret, G. Gaudin, and P. Gambardella, *Phys. Rev. B* **89**, 214419 (2014).
- [43] B. K. Nikolić, S. Souma, L. P. Zârbo, and J. Sinova, *Phys. Rev. Lett.* **95**, 046601 (2005).
- [44] B. K. Nikolic, L. P. Zarbo, and S. Souma, *Phys. Rev. B* **73**, 075303 (2006).
- [45] *Electron Scattering in Solid Matter: A Theoretical and Computational Treatise*, edited by J. Zabloudil, Springer Series in Solid-State Sciences Vol. 147 (Springer, New York, 2005).
- [46] M. Gradhand, M. Czerner, D. V. Fedorov, P. Zahn, B. Y. Yavorsky, L. Szunyogh, and I. Mertig, *Phys. Rev. B* **80**, 224413 (2009).
- [47] M. Gradhand, D. V. Fedorov, P. Zahn, and I. Mertig, *Phys. Rev. B* **81**, 020403(R) (2010).
- [48] C. Heiliger, M. Czerner, B. Y. Yavorsky, I. Mertig, and M. D. Stiles, *J. Appl. Phys. (Melville, NY)* **103**, 07A709 (2008).
- [49] C. Franz, M. Czerner, and C. Heiliger, *J. Phys.: Condens. Matter* **25**, 425301 (2013).
- [50] C. E. Mahr, M. Czerner, and C. Heiliger, *Phys. Rev. B* **96**, 165121 (2017).
- [51] S. Datta, *Electronic Transport in Mesoscopic Systems* (Cambridge University Press, Cambridge, 1995).
- [52] C. Herschbach, M. Gradhand, D. V. Fedorov, and I. Mertig, *Phys. Rev. B* **85**, 195133 (2012).
- [53] Y. V. Sharvin, *Zh. Eksp. Teor. Fiz.* **48**, 984 (1965) [*Sov. Phys. JETP* **21**, 655 (1965)].
- [54] H. L. Wang, C. H. Du, Y. Pu, R. Adur, P. C. Hammel, and F. Y. Yang, *Phys. Rev. Lett.* **112**, 197201 (2014).
- [55] J. Qiao, J. Zhou, Z. Yuan, and W. Zhao, *Phys. Rev. B* **98**, 214402 (2018).
- [56] M.-H. Wu, H. Rossignol, and M. Gradhand, *Phys. Rev. B* **101**, 224411 (2020).
- [57] See Supplemental Material at <http://link.aps.org/supplemental/10.1103/PhysRevB.104.054402> for an overview of accumulations of all the small systems as well as accumulations for the larger systems of Cu, Pt, and U. Furthermore, the Fermi surfaces with color encoded group velocities are shown for all systems.
- [58] O. Gueckstock, L. Nádovrník, M. Gradhand, T. S. Seifert, G. Bierhance, R. Rouzegar, M. Wolf, M. Vafaei, J. Cramer, M. A. Syskaki, G. Woltersdorf, I. Mertig, G. Jakob, M. Kläui, and T. Kampfrath, *Adv. Mater. (Weinheim)* **33**, 2006281 (2021).
- [59] E. Sagasta, Y. Omori, M. Isasa, M. Gradhand, L. E. Hueso, Y. C. Niimi, Y. Otani, and F. Casanova, *Phys. Rev. B* **94**, 060412(R) (2016).
- [60] T. D. Skinner, K. Olejník, L. K. Cunningham, H. Kurebayashi, R. P. Champion, B. L. Gallagher, T. Jungwirth, and A. J. Ferguson, *Nat. Commun.* **6**, 6730 (2015).